J Mol Model (2012) 18:4007–4012
DOI 10.1007/s00894-012-1398-z

ORIGINAL PAPER

Modeling the interaction of seven bisphosphonates with the hydroxyapatite(100) face

Chunyu Chen · Mingzhu Xia · Lei Wu · Chao Zhou · Fengyun Wang

Received: 3 October 2011 / Accepted: 1 March 2012 / Published online: 27 March 2012

Abstract The interaction of seven pamidronate bisphosphonate (Pami-BPs) and its analogs with the hydroxyapatite (HAP) (100) surface was studied using density functional theory (DFT) and molecular dynamic (MD) methods. Partial Mulliken oxygen atomic charges in protonated structures were calculated at the level of B3LYP/6-31G*. The MD simulation was performed using the Discover module of Material Studio by compass force field. The results indicate the abilities of donating electrons of the oxygen atoms of the phosphate groups that are closely associated with the antiresorptive potency. The binding energies, including vdw and electrostatic, are used to discuss the mechanism of antiresorption. The results of calculations show that the strength of interaction of the HAP (100) face with the bisphosphonates is $N_4>N_6>N_7>N_5>N_3>N_2>N_1$ according to their experimental pIC_{50} values.

Keywords Bisphosphonates · Hydroxyapatite · Density functional theory · Molecular dynamic · Antiresorption

Introduction

Hydroxyapatite (HAP, $[Ca_{10}(PO_4)_6(OH)_2]$) is a significant component of human bone and tooth-enamel [1], with an amount of approximately 65 wt% HAP in bone and more than 95 wt% in tooth-enamel. HAP has excellent biocompatibility and chemical stability. Bisphosphonates (BPs) are currently the most important and effective class of antiresorptive drugs available in the treatment of degenerative bone diseases such as Paget's disease, post-menopausal osteoporosis and tumour-associated osteoporosis [2, 3].

BPs, which are inexistent in nature, are synthetic analogues of pyrophosphate (PPi) consisting of two phosphate groups linked by a central carbon atom instead of the original P–O–P backbone structure and two covalently bonded side chains (R_1 and R_2) (Fig. 1) [2, 4]. BPs have the ability to bind avidly to divalent metal ions such as Ca^{2+} due to the presence of the P–C–P backbone linkage, which can explain why BPs appear to inhibit osteoclast-mediated bone resorption (Fig. 2). Under normal physiological conditions, osteoblasts and osteoclast activity is always in a dynamic equilibrium of mutual adjustment, whilst osteoblasts have a positive stimulatory effect on osteoclast activity [5].

A considerable amount of research has focused on the interaction of HAP with H_2O [1], citric acid [6], proteins [7] and polymers [8], but not much effort has been put into studying the adsorption of BPs on HAP through computational chemistry and molecular modeling. Robinson et al. [9] studied the interaction of MDP (R_1=R_2=H), HEDP (R_1=OH, R_2=CH_3), APD [R_1=OH, R_2=$(CH_2)_2NH_3^+$], alendronate (R_1=OH, R_2=$(CH_2)_3NH_3^+$) and neridronate (R_1=OH, R_2=$(CH_2)_5NH_3^+$) with the (001), (010) and (100) faces of HAP [9, 10]. The results show non-bonded interactions dominate where there is a high dielectric constant, whereas electrostatic interactions play a very important role

C. Chen · M. Xia · L. Wu · C. Zhou · F. Wang (✉)
Institute of Industrial Chemistry,
Nanjing University of Science and Technology,
Nanjing 210094, China
e-mail: ici_njust@yahoo.cn

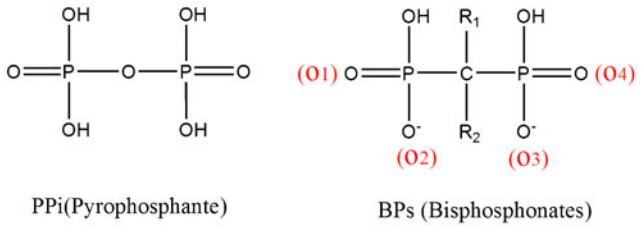

Fig. 1 Common structure of bisphosphonates

when the dielectric constant is low. The exothermic interaction energy changes with molecular volume (MDP< HEDP<APD<alendronate) except for neridronate because the long amino side chain folds in on itself in agreement with the data in vivo.

Early work examined the interaction of three phosphonates (EDTMP, HDTMP and DTPMP) with the surfaces of calcite [11]; and these interactions have also been studied by molecular dynamic simulation using Materials Studio [12] v3.0 (Accelrys, San Diego, CA) under compass [13] force field. The results showed the Ca–O ($–PO_3^{2-}$) distance after dynamic simulations was less than 2.5 Å, in accordance with the length of the Ca–O bond, implying that phosphonates should have a high affinity for calcite [14]. This work investigated the mechanism of the interaction of pamidronate bisphosphonate (Pami-BP) and its analogs with the HAP (100) face as a model of bone by density functional theory (DFT) [15] using quantum chemical calculation and molecular dynamic (MD) simulation in an alkalescent aquatic environment of body. To facilitate comparison with the seven bisphosphonates (N1–N7), the code designations shown in Fig. 3 were used.

Methods

Quantum chemical calculation

The geometry structures of the seven bisphosphonates were optimized using the Gaussian 03 procedure by means of DFT methods. Partial oxygen atomic Mulliken charges are assigned from B3LYP/6-31G* single point calculation at the geometry. The structures (seen in Fig. 3) were protonated referring to experimental data because of the pH values (range 7.2–76) in an alkalescent aquatic environment.

Molecular dynamic simulation

We simulated seven protonated nitrogen-containing bisphosphonates (N1–N7) onto the HAP (100) face in a water environment using Materials Studio v3.0 (MS) under compass force field [16] as in previous studies. Simulation details of MD are shown in Table 1.

The strength of interaction of the surface with the inhibitor is shown by the binding energy, calculated according to Eq. (1).

$$\Delta E = E_{sysrem} - \left(E_{surface+water} + E_{inhibitor+water} - E_{water}\right)$$
$$E_{binding} = -\Delta E \quad (1)$$

where E_{system} is the total energy of the simulation system, $E_{\text{surface+water}}$ is the energy of the surface with water, $E_{\text{inhibitor+water}}$ is the energy of the free inhibitor molecule with water, and E_{water} is the energy of the free water molecule after calculation.

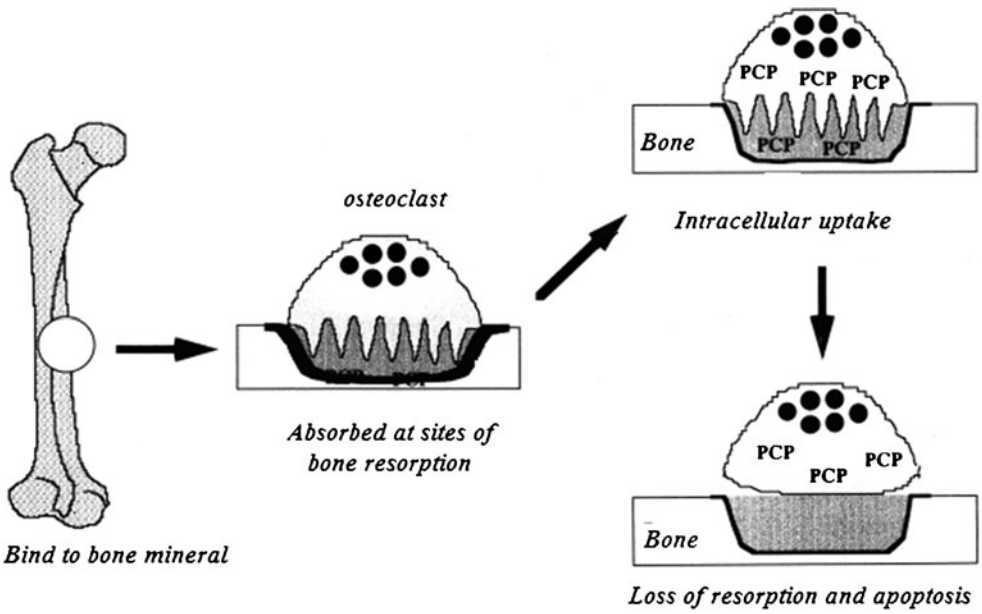

Fig. 2 Route of bisphosphonates preventing bone resorption by osteoclasts

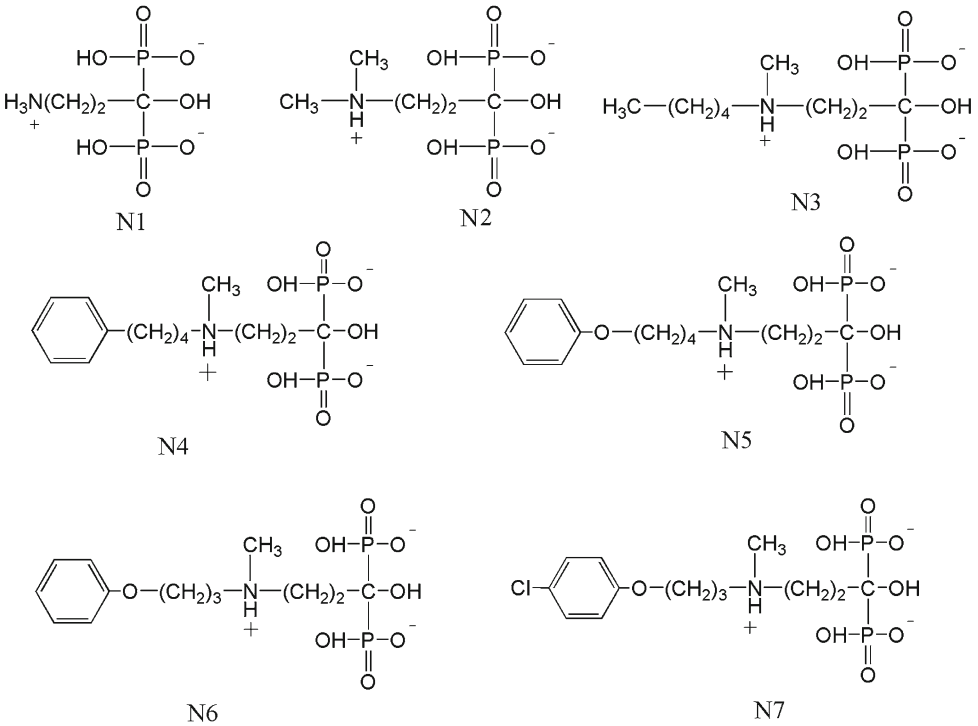

Fig. 3 Molecular structure of 7 protonated molecules (N1–N7)

Results and discussion

Mulliken oxygen atomic charges

The four oxygen atomic charges (marked in Fig. 1) obtained in this work are summarized in Table 2; the interaction of the oxygen atom in the $–PO_3H^-$ group with the Ca^{2+} of HAP becomes stronger along with the increase of oxygen atomic negative charges. This result shows that the oxygen atoms in the $–PO_3H^-$ group have a mass of negative charges inducing the strong interaction of bisphosphonates with HAP. The results also show clearly that the average of the oxygen atomic charge of N4 is 0.6819e, which is the most among the seven compounds. Based on the data, we conclude that N4 is likely to be the greatest inhibitor of HAP growth. Comparing the charges of N1, N2 and N3, in which the R_1 and R_2 side chains are a hydroxyl (−OH) group and a nitrogen-containing alkyl chain, respectively, it was found that N3 is energetically most favorable. The inhibition effect of N1 is possibly weakest because of having the shortest alkyl side chain length. Both N6 and N7 have almost the same structure except for the chlorine linked to the phenyl group. The presence of the chlorine group leads to a decrease in the charge on the oxygen atoms.

Hydroxyapatite

HAP has a hexagonal structure (Fig. 4a), with a P63/m space group [17], where the simulative dimensions of the unit cell are $a=b=0.943$ nm and $c=0.688$ nm, $\alpha=\beta=90°$,

Table 1 Simulation details of molecular dynamic (MD) simulation

Simulation parameter	Value	Simulation parameter	Value
Force field	Compass	Summation method[a]	Atom based / customized
Non-bond	Vdw, Coulomb	Simulation temperature	310 K
Ensemble	NVT	Minimization	Smart minimizer
Thermostat	Berendsen	Convergence level	Medium
Time step	1 fs	Maximum iterations	5,000
Frame output	100	Energy deviation	5,000 kCal/mol
Dynamic time	100 ps	Number of steps	100,000
Cut-off distance	0.95 nm	Production steps	15 ps
Dielectric constant	75.0	Decay constant	0.1 ps

[a]Summation methods were applied to calculate non-bond interactions: “Atom based” for van der Waals interactions and “Customized” for coulomb interactions

Table 2 Optimized Mulliken oxygen atomic charges of protonated bisphosphonate groups (unit e)

N1	N2	N3	N4	N5	N6	N7
O1-0.7089	O1-0.6892	O1-0.6901	O1-0.6972	O1-0.6741	O1-0.6785	O1-0.6596
O2-0.6354	O2-0.6738	O2-0.6733	O2-0.6449	O2-0.6627	O2-0.6741	O2-0.6589
O3-0.7007	O3-0.6642	O3-0.6634	O3-0.7015	O3-0.6819	O3-0.6793	O3-0.6780
O4-0.5706	O4-0.6700	O4-0.6715	O4-0.6839	O4-0.6672	O4-0.6878	O4-0.6571
−0.6539	−0.6739	−0.6746	−0.6819	−0.6715	−0.6799	−0.6634

γ=120°. The thermodynamic morphology of the HAP crystal was obtained using the Bravais-Friedel-Donnay-Harker (BFDH) morphology prediction method of MS, shown in Fig. 4b, where the (100) and (101) surfaces are the highest probability faces according to morphology found in previous work [18, 19]. Although the (001) face was thought by Wierzbicki and Cheung [18] to occur frequently in the uninhibited growth of HAP, we think this surface is covered due to rapid growth without inhibition. In this work, the (100) surface has been designated, then minimized using Newton under the periodic boundary conditions with a non-bond cut-off distance of 9.5 Å.

Interaction of protonated bisphosphonates with the HAP (100) face in water

In order to conform the actual aqueous medium of body, the movement and effect of water in the total system must be considered by means of setting the permittivity (dielectric constant, ε) and adding water molecules. In this paper, ε is set of 75.0 and a mass of water molecules are added to each surface of HAP according to the 37°C water environment of the human body [20].

Figure 5 shows clearly that all of the phosphate groups point towards the HAP (100) surfaces instead of water molecules; nevertheless, the R_2 side chains point away from the surfaces. The results suggest that the seven bisphosphonates interact well with the HAP (100) surface on account of the oxygen atoms of its phosphate group contacting well with calcium ions on the surface, whereas the R_2 side chains have little interaction with HAP. The Ca–O (P) distances are all less than 2.5 Å, in accordance with the Ca–O bond length found experimentally. In the HAP (100) face, the Ca_1 ions are the outermost components of the crystal. The Ca_1 ions were found to be four-fold coordinated equally by bisphosphonate oxygen atoms. The radial distribution functions taken for the distances between the Ca_1 ions and the oxygen atoms of the bisphosphonates are shown in Fig. 6. The interaction of the seven bisphosphonates with HAP is mainly similar. The strongest peak occurs at a distance of about 2.5 Å, showing the formation of an electrovalent bond between the Ca ion and oxygen atom. For further analysis of the effectiveness of antiresorption, we consider the binding energy of interaction between the seven phosphonates ligands (N1–N7) and HAP in the aqueous phase separately (listed in Table 3). This indicates clearly that the energy of interaction is dominated by electrostatic interaction, with a dielectric constant of 75.0, whereas van der Waals interactions play only a very minor role in the non-bonded interaction [21].

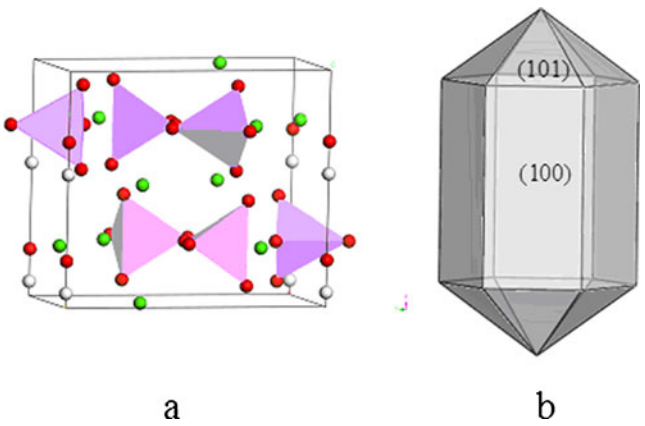

Fig. 4 The unit cell and calculated equilibrium morphology of the hydroxyapatite (HAP) crystal

Based on the data in Table 3, the interaction energy is exothermic and the effectiveness of antiresorption is N4>N6>N7>N5>N3>N2>N1 in agreement with experimental antiresorptive potency (PIC_{50} values) [22]. When the R_1 side chain is an –OH group, bisphosphonates increase their ability to chelate calcium ions. Because the R_1 side chain in the seven bisphosphonates is the same, the R_2 side chain structures play a decisive role in antiresorption. Compared with the energy of N1, N2 and N3, the antiresorptive potency was increased by the insertion of an alkyl chain in the R_2 side chain. Importantly, potency varies with the length of alkyl chain, which induces the antiresorptive effect: N3>N2>N1. The potency of the amino-alkyl bisphosphonates is increased further by insertion of an aryl group because the negative charges of benzene can improve the performance of anti-bone resorption. Hence, N4 appears more potent than N3. The addition of a chloride ion leads to a decrease in the antiresorptive potency because chloride ions have a strong electron-withdrawing effect. Therefore, the potency is N6>N7.

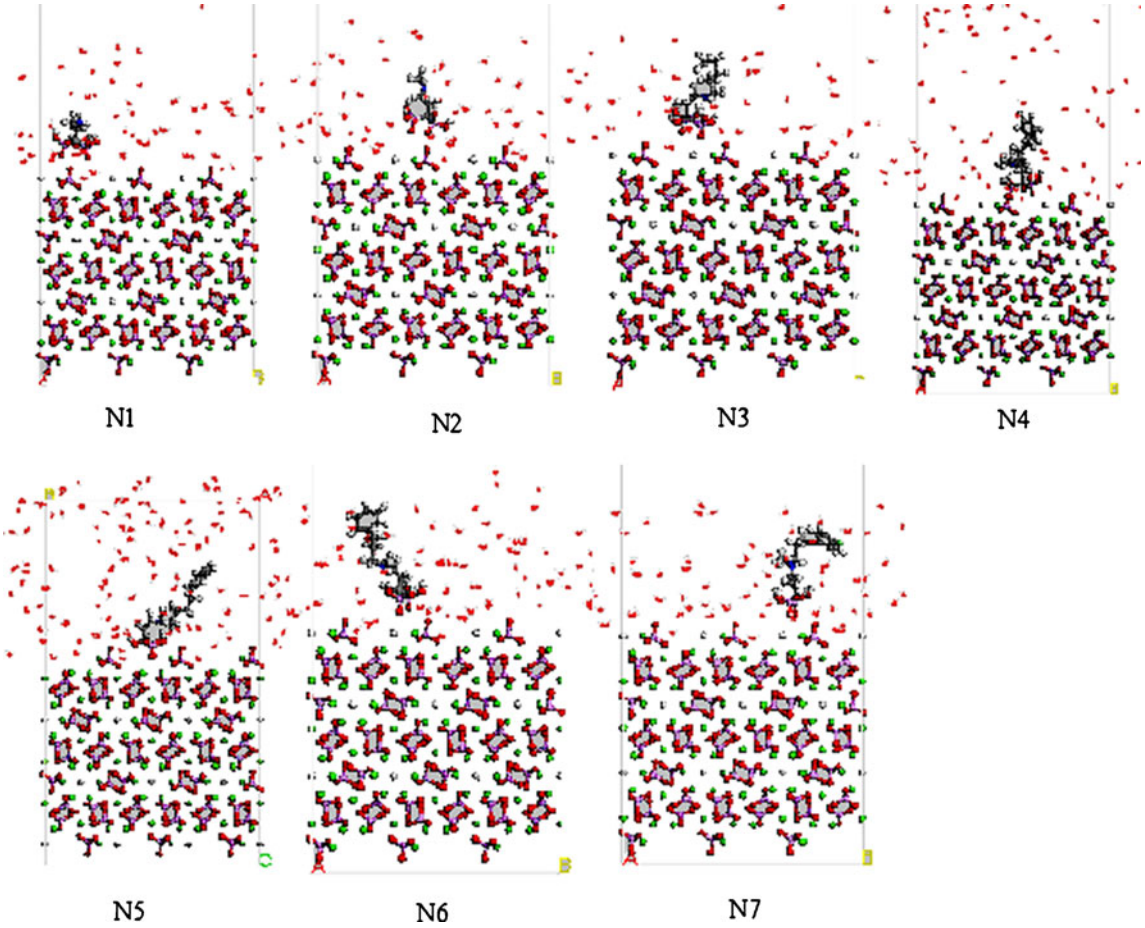

Fig. 5 Side views of seven compounds adsorbing on the HAP (100) surface. *Green* Ca, *grey* C, *red* O, *purple* P, *blue* N, *yellow* S, *light green* Cl, *white* H

Conclusions

This work presents research into the molecular interaction of bisphosphonate acids with the HAP (100) surface using DFT and MD methods. In summary, the presence of bisphosphonates has a significant effect on anti-bone resorption. The results lead to the conclusion that the antiresorptive potency of seven bisphosphonates is N4>N6>N7>N5>N3>N2>N1 due to the different R_2 side chains, and this is in accordance with experimental antiresorptive ability PIC_{50} values. Future work will focus on the interaction of bisphosphonates with the HAP (101) and (001) faces in the presence of water.

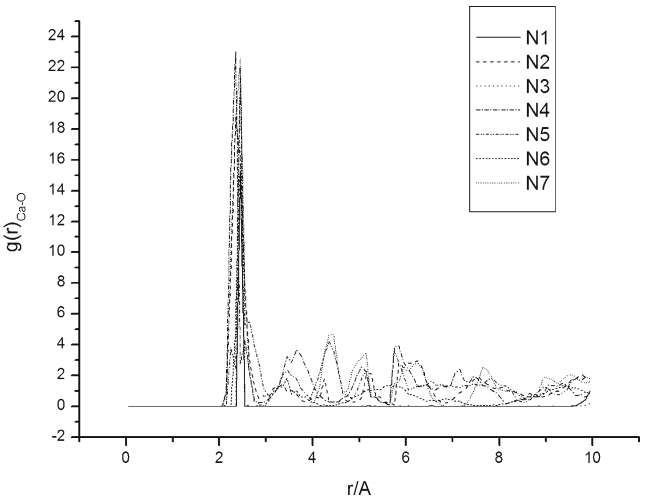

Fig. 6 Pair correlation functions of the calcium ions of HAP(100) surface and oxygen atoms of the molecules

Table 3 pIC_{50} values and binding energies of seven compounds with hydroxyapatite (HAP) (100) surface (unit eV)

Molecule	pIC_{50}	$\triangle E_{vdw}$	$\triangle E_{coulomb}$	$\triangle E$
N1	6.864	4.16	44.23	−48.40
N2	7.520	5.13	45.17	−50.31
N3	7.667	3.27	47.72	−51.00
N4	8.979	4.45	73.82	−78.28
N5	7.997	4.52	48.89	−53.42
N6	8.885	5.52	69.66	−75.19
N7	8.506	4.24	68.66	−72.91

Acknowledgments This work is supported by the Institute of Industrial Chemistry, Nanjing University of Science & Technology. The help of Dr. Wang in performing the simulations is kindly acknowledged.

References

1. Zahn D, Hochrein O (2003) Phys Chem Chem Phys 5:4004–4007
2. Lin JH (1996) Bone 18(2):75–85
3. Coxon FP, Thompson K, Rogers MJ (2006) Curr Opin Pharmacol 6:307–312
4. Cukrowski I, Popović L, Barnard W, Paul SO, van Rooyen PH, Liles DC (2007) Bone 41:668–678
5. Yu X, Schøller J, Foged NT (1996) Bone 19(4):339–345
6. Filgueiras MRT, Mkhonto D, de Leeuw NH (2006) J Cryst Growth 294:60–68
7. Rimola A, Corno M, Zicovich-Wilson CM, Ugliengo P (2008) J Am Chem Soc 130(48):16181–16183
8. Bhowmik R, Katti KS, Katti D (2007) Polymer 48(2):664–674
9. Robinson J, Cukrowski I, Marques HM (2006) J Mol Structure 825:134–142
10. Neves M, Gano L, Pereira N, Costa MC, Costa MR, Chandia M, Rosado M, Fausto R (2002) Nucl Med Biol 29:329–338
11. Alder BJ, Wainwright TE (1957) Chem Phys 27:1208–1209
12. Materials Studio 4 (2007) 2 Discover/Accelrys, San Diego, CA
13. Ramachandran S, Tsai BL, Blanco M (1996) Langmuir 12 (26):6419–6428
14. Chen CY, Xia MZ, Wang FY (2010) Advanced Mater Res 154–155:437–442
15. Perdew JP (1986) Phys Rev B 33(12):8822–8824
16. Pedone A, Corno M, Civalleri B, Malavasi G, Menziani MC, Segre U, Ugliengo P (2007) J Mater Chem 17:2061–2068
17. Posner AS, Perloff A, Diorio AF (1958) Acta Crystallogr 11:308
18. Wierzbicki A, Cheung HS (1998) J Mol Model 454:287–297
19. Pan HH, Tao JH, Xu XR, Tang RK (2007) Langmuir 23:8972–8981
20. Leeuw NH de, Rabone JAL (2007) J Cryst Eng Commun 9:1178–1186
21. Zieba A, Sethuraman G, Perez F, Nancollas H, Cameron D (1996) Langmuir 12(11):2853–2858
22. Kotsikorou E, Oldfield E (2003) J Med Chem 46:2932–2944